Predictability in systems with many characteristic times: The case of turbulence

E. Aurell

Department of Mathematics, Stockholm University, S-106 91 Stockholm, Sweden

G. Boffetta

Istituto di Fisica Generale, Università di Torino, Via Pietro Giuria 1, I-10125 Torino, Italy

A. Crisanti

Dipartimento di Fisica, Università di Roma "La Sapienza," Piazzale Aldo Moro 2, I-00185 Roma, Italy

G. Paladin

Dipartimento di Fisica, Università dell'Aquila Via Vetoio, Coppito I-67100 L'Aquila, Italy

A. Vulpiani

Dipartimento di Fisica, Università di Roma "La Sapienza," Piazzale Aldo Moro 2, I-00185 Roma, Italy

In chaotic dynamical systems, an infinitesimal perturbation is exponentially amplified at a rate given by the inverse of the maximum Lyapunov exponent λ. In fully developed turbulence, λ grows as a power of the Reynolds number. This result could seem to be in contrast to phenomenological arguments suggesting that, as a consequence of "physical" perturbations, the predictability time is roughly given by the characteristic lifetime of the large scale structures, and hence is independent of the Reynolds number. We show that such a situation is present in generic systems with many degrees of freedom, since the growth of a noninfinitesimal perturbation is determined by the cumulative effects of many different characteristic times and is unrelated to the maximum Lyapunov exponent. Our results are illustrated in a chain of coupled maps and in a shell model for the energy cascade in turbulence.

PACS number(s): 47.27.Gs, 05.45.+b

I. INTRODUCTION

After the seminal work of Lorenz [1], it is well understood that the predictability of the state of a system ruled by a deterministic evolution law has severe limitations in the presence of deterministic chaos. In systems with sensitive dependence on the initial condition one has an exponential divergence of the distance $\delta \mathbf{x}$ between two initially close trajectories, i.e.,

$$|\delta \mathbf{x}(t)| \simeq |\delta \mathbf{x}(0)| \, e^{\lambda t}, \tag{1}$$

where λ is the maximum Lyapunov exponent [2]. Consequently, if $|\delta \mathbf{x}(0)| = \delta_0$ and one accepts a maximum tolerance $\delta_{\max}$ on the knowledge of the state of the system, (1) implies that the system is predictable up to a time

$$T \sim \frac{1}{\lambda} \ln \left(\frac{\delta_{\max}}{\delta_0} \right). \tag{2}$$

Equation (2) gives only a first rough answer to the problem since it does not take into account some important features of chaotic systems. Indeed to study the predictability of a generic dynamical system one has to consider the following nontrivial aspects.

(a) The Lyapunov exponent λ is a global quantity: it measures the average exponential rate of divergence of nearby trajectories. In general there are finite-time fluctuations of this rate and it is possible to define an "instantaneous" rate γ, called the effective Lyapunov exponent [3], which depends on the particular point of the trajectory $\mathbf{x}(t)$ where the perturbation is performed. In the same way, the predictability time T fluctuates, following the γ variations.

(b) In dynamical systems with many degrees of freedom, the interactions among different parts of the system play an important role on the growth of a perturbation. The statistics of the effective Lyapunov exponent is not sufficient to characterize the growth of infinitesimal perturbations and one has to analyze the behavior of the tangent vector $\mathbf{z}(t)$, i.e., of the direction along which an infinitesimal perturbation grows, see, e.g., [4]. Moreover, if one is interested in the behavior of a perturbation concentrated on certain degrees of freedom, e.g., small length scales in weather forecasting, and in a prediction on the evolution of other degrees of freedom, e.g., large length scales, a relevant quantity is the time T_R necessary for the tangent vector to relax on the time-dependent eigenvector $\mathbf{e}(t)$ of the stability matrix, corresponding to the maximum Lyapunov exponent. If the perturbations are small enough, i.e., $\delta \mathbf{x}$ is proportional to the tangent vector, one has that

$$T \sim T_R + \frac{1}{\lambda} \ln \frac{\delta_{\max}}{\delta_0}, \qquad (3)$$

where in general T_R may depend on δx. So the mechanism of transfer of the error δx through the degrees of freedom of the system could be more important than the rate of divergence of nearby trajectories [5].

(c) In systems with many characteristic times, such as the eddy turnover times in fully developed turbulence, if the perturbation is not infinitesimal, or if the threshold of accepted error is not small, T is determined by the detailed mechanism of transfer due to the nonlinear effects in the evolution equation for δx. In this case, the predictability time might have no relation with the Lyapunov exponent and T depends in a nontrivial way on the details of the system.

The aspects (a) and (b) have been studied in previous works [5–7]. In this paper we mainly address point (c). We investigate the predictability problem for noninfinitesimal perturbations in the framework of two models: a system of coupled maps and a shell model for the energy cascade in three-dimensional turbulence.

The paper is organized as follows. In Sec. II we discuss some phenomenological results in fully developed turbulence. In Sec. III the predictability problem is discussed in a system of coupled maps, using analytic methods supported by some numerical investigations. Section IV analyzes the more realistic case of a shell model of turbulence by both numerical simulations and closure approximations. In Sec. V we discuss the physical relevance of our results and open problems.

II. SOME RESULTS FOR THE PREDICTABILITY IN FULLY DEVELOPED TURBULENCE

In three-dimensional fully developed turbulence, the inverse maximum Lyapunov exponent is roughly proportional to the smallest characteristic time of the system, the turnover time τ of eddies of the size of the Kolmogorov length η. The argument, due to Ruelle [8], is the following. The Kolmogorov theory predicts that the longitudinal velocity difference at distance $\ell = |\mathbf{r}|$ scales as

$$v(\ell) \equiv |\mathbf{v}(\mathbf{x} + \mathbf{r}) - \mathbf{v}(\mathbf{x})| \sim \epsilon^{1/3} \ell^{2/3} \sim V \left(\frac{\ell}{L}\right)^{1/3}, \quad (4)$$

where V and L are the typical velocity and length of the energy-containing eddies, and ϵ is the mean rate of energy dissipation.

The nonlinear transfer of energy is stopped at the Kolmogorov scale η where viscosity ν is able to compete with the convective term, i.e., $\nu \sim \eta v(\eta)$, thus from (4) we have

$$\eta \sim L \, \mathrm{Re}^{-3/4}, \qquad (5)$$

where $\mathrm{Re} = VL/\nu$ is the Reynolds number. The corresponding turnover time is

$$\tau(\eta) \sim \frac{\eta}{v(\eta)} \sim T_0 \left(\frac{\eta}{L}\right)^{2/3}, \qquad (6)$$

where $T_0 = L/V$ is the lifetime of the large scale disturbances.

These dimensional relations imply that the maximum Lyapunov exponent scales with Re as

$$\lambda \sim \frac{1}{\tau(\eta)} \sim \frac{1}{T_0} \mathrm{Re}^{1/2}. \qquad (7)$$

Taking into account the intermittency one expects that the presence of quiescent quasilaminar periods changes the chaotic features of the fluid flow. The intermittency of energy dissipation can be described by introducing a spectrum of singularities h of the velocity gradients [9], i.e., assuming a local scaling invariance so that in any point $\mathbf{x}$ of the fluid $v(\ell) \sim \ell^{h(\mathbf{x})}$. In the framework of the multifractal approach, one thus finds [7]

$$\lambda \sim \frac{1}{T_0} \mathrm{Re}^\alpha \quad \text{with } \alpha = \max_h \left[\frac{D(h) - 2 - h}{1 + h} \right], \qquad (8)$$

where $D(h)$ is the fractal dimension of the set of fluid points characterized by a given singularity h. The value of α depends on $D(h)$. By using the function $D(h)$ obtained by fitting the exponents ζ_q of the velocity structure functions with the random beta model [10], one has $\alpha = 0.459...$, slightly smaller than the Ruelle prediction $\alpha = 0.5$, see (7).

Relations (2) and (8) tell us that considering a very small perturbation at $t = 0$ and a very small tolerance $\delta_{\max}$, the predictability time vanishes as the Reynolds number increases, as verified in recent numerical simulations of the shell model (see Sec. IV) [6].

On a very different ground, without considering the exponential growth of infinitesimal disturbances, Lorenz [11], see also [12] and [13], proposed a phenomenological approach to the predictability problem in turbulence. Consider wave numbers around k with corresponding typical spatial scale $\ell \sim k^{-1}$. The time $\tau(k)$ for a perturbation at wave number $2k$ to induce a complete uncertainty on the velocity field on the wave number k is assumed to be proportional to the typical eddy turnover time at scale ℓ, from (4):

$$\tau(\ell) \sim \frac{\ell}{v(\ell)} \sim T_0 \left(\frac{\ell}{L}\right)^{2/3}. \qquad (9)$$

An incertitude $O(v(\eta))$ propagates through an inverse cascade from the Kolmogorov scale $\eta \sim k_d^{-1}$ up to the scale of the energy-containing eddies $L \sim k_0^{-1}$. The predictability time on the large scales is therefore

$$T = \sum_{n=0}^{N} \tau(2^n \eta), \qquad (10)$$

where $N = \log_2(k_d/k_0) \sim \log_2 \mathrm{Re}$. The geometric series (10) is dominated by the term $n = N$ so that T is practically independent of Reynolds number:

$$T \sim T_0 \sim L/V. \tag{11}$$

It is worth remarking that closure approximations [12,13] allow one to write down simple equations for the evolution of disturbances in turbulent flows and fully confirm these results. In Appendix B, we derive this type of equation in the simplified framework of the shell model, but there are no conceptual differences with the analogous derivation in the case of the Navier-Stokes equations.

The Lorenz picture of an inverse cascade of a perturbation also permits us to estimate the growth of a perturbation at intermediate times. Indeed, after a time t, a perturbation localized on the Kolmogorov length scale is expected to affect an eddy of size ℓ_t such that its turnover time is $\tau(\ell_t) \sim t$. It follows [14], see (9),

$$\ell_t \sim L \left(\frac{t}{T_0}\right)^{3/2}. \tag{12}$$

Let us indicate by v the reference velocity field and by v' the perturbed field. The size of the difference $\delta v(t)$ between two velocity fields at time t can be estimated as the typical velocity of a disturbance at scale ℓ_t, so that from (4) and (12)

$$|\delta v(t)| \sim v(\ell_t) \sim V \sqrt{t/T_0}. \tag{13}$$

Perturbations grow as square root of time. Let us stress again that such perturbations cannot be considered infinitesimal so that the inverse cascade picture is not in contrast with the exponential amplification of errors on initial conditions that is present in chaotic dynamical systems.

There are two main predictions of the Lorenz approach: predictability time on large scale independent of Reynolds number and growth of perturbations as a power of time instead of an exponential.

In the next sections we use the theory of dynamical systems with many degrees of freedom to argue that while the former is correct, the latter is a too rough description of the real behavior of $\delta v(t)$.

III. PREDICTABILITY IN A CHAIN OF COUPLED MAPS

In this section we discuss the predictability problem in a system of coupled maps each with a different time scale. This is an idealized situation where each degree of freedom has a chaotic dynamics with its own characteristic time and it is coupled to the other degrees of freedom by a weak local interaction. Our toy model can be considered the prototype for physical situations where one can separate the evolution on different scales. Despite its simplicity, it displays nontrivial properties which enlighten the behavior of more complex systems.

The system is given by a chain of chaotic coupled maps

$$x_1(t+1) = (1 - \epsilon)g_1(x_1(t)) + \epsilon f(x_2(t)),$$
$$x_2(t+1) = (1 - \epsilon)g_2(x_2(t)) + \epsilon f(x_3(t)),$$
$$\vdots \tag{14}$$
$$x_{N-1}(t+1) = (1 - \epsilon)g_{N-1}(x_{N-1}(t)) + \epsilon f(x_N(t)),$$
$$x_N(t+1) = g_N(x_N(t)),$$

where the N variables x_k are defined on the interval $I = [0, 1]$, ϵ is the coupling constant, and g_k and f are functions of I into itself. In order to mimic the energy cascade of turbulent flow, we assume that the function g_k represents the evolution law of an eddy of size l_k in the absence of interactions. In this context, x_k can be regarded as the velocity difference of the eddies on the octave of length scale $l_k = L_0 2^{-k}$. The evolution is chaotic with a Lyapunov exponent proportional to the inverse of the eddy turnover time τ_k. The simplest possible choice for $g_k(x)$ is the piecewise linear map

$$g_k(x) = e^{\lambda_k} x, \quad \text{mod } 1. \tag{15}$$

This choice allows for a simple analytical treatment of the problem.

In order to mimic the phenomenology of fully developed turbulence, using dimensional arguments and (9), we choose the eddy turnover time τ_k so that the Lyapunov exponent is

$$\lambda_k = \frac{1}{T_0} 2^{2/3(k-1)}. \tag{16}$$

The coupling parameter ϵ is small and constant for each scale, although more realistic models could consider scale-dependent couplings. The form of $f(x)$—the term representing the local interaction between eddies—does not affect the qualitative results. We have considered two possibilities: $f(x) = x$ and $f(x) = x^2$.

In order to study the predictability, the system (14) has been integrated with two different initial conditions $\mathbf{x}(0)$ and $\mathbf{x}'(0)$ differing on the smallest scale, $\Delta_k(0) \equiv x'_k(0) - x_k(0) = \delta_{k,N}\delta_0$. The initial incertitude is thus confined to the smallest and fastest scale x_N while we want to forecast the behavior of the system at the largest scale x_1.

Because time scales are well separated, we expect that at the beginning the uncertainty in the system is driven by the fastest scale x_N and the error at any scale grows with the smallest characteristic time

$$\Delta_k(t) \sim \epsilon^{N-k} e^{\lambda_N t}\delta_0, \tag{17}$$

where the power of ϵ is due to the locality of the interactions. The behavior (17) will last up to the time T_N at which the perturbation at small scale saturates, i.e., $\Delta_N = \Delta_{\text{sat}}$. Then a second regime driven by the variable x_{N-1}, which has now the fastest exponential growth of errors, sets in. When this second regime holds, the incertitudes at scales $k \leq N - 1$ grows as $\sim e^{\lambda_{N-1}t}$ until, at time T_{N-1}, the variable x_{N-1} saturates and x_{N-2} dominates, and so on. Such an argument suggests that a perturbation Δ_1 at the largest scale x_1 follows different

exponential laws with rates λ_k $(k = 1, \ldots, N)$ in each different regime, with a global (envelope) evolution which appears very similar to a power law.

Figure 1 shows the error observed at large scale Δ_1 as a function of time in a numerical experiment realized with a chain of $N = 10$ maps. The coupling function is chosen linear, $f(x) = x$, the coupling parameter is $\epsilon = 10^{-4}$, and the largest characteristic time is $T_0 = 200$. The initial conditions are random and the initial perturbation on the small scale is $\delta_0 = 10^{-8}$. In a typical chaotic system where there is only one characteristic time scale, e.g., the Lorenz model, the exponential regime for the growth of a perturbation is recognizable, as straight lines in the linear-logarithmic plot, for a wide range of values of $|\delta\mathbf{x}(t)|$. On the contrary from Fig. 1 we see that the smaller scale dominates the exponential regime only for short time.

This behavior can be well understood by means of a quasilinear analysis which also allows for some analytical estimates. The evolution with (15) and linear $f(x)$ leads to a linear evolution for the perturbation,

$$\boldsymbol{\Delta}(t + 1) = A\,\boldsymbol{\Delta}(t), \tag{18}$$

where A is the $N \times N$ Jacobian matrix

$$A = \begin{pmatrix} l_1 & \epsilon & 0 & \ldots & 0 & 0 \\ 0 & l_2 & \epsilon & \ldots & 0 & 0 \\ \vdots & \vdots & \vdots & \ddots & \vdots & \vdots \\ 0 & 0 & 0 & \ldots & 0 & l_N \end{pmatrix}. \tag{19}$$

Let us denote with T_k the time at which scale k saturates, i.e., $\Delta_k(T_k) = 1$, and with M_k the period (number of steps) during which scale k dominates the dynamics,

i.e., $M_k = T_k - T_{k+1}$. If we suppose that the main contribution to the growth of perturbations during period M_k is given by the faster scale Δ_k, which is correct whenever ϵ is very small, we can write for any $i < k$

$$\Delta_i(T_k) = \Delta_i(T_{k+1}) + (A^{M_k})_{i,k}\Delta_k(T_{k+1}) \tag{20}$$

while $\Delta_i(T_k) = \Delta_{\text{sat}}$ for $i \geq k$. The matrix A^M can be easily computed and at the leading order is given by

$$(A^M)_{i,k} = \epsilon^{k-i}\frac{e^{M\lambda_k} - e^{M\lambda_i}}{e^{\lambda_k} - e^{\lambda_i}}. \tag{21}$$

From (20) and (21), and using the fact that $e^{M_k\lambda_k}\Delta_k(T_{k+1}) \sim \Delta_{\text{sat}}$, we obtain

$$M_k = \frac{1}{\lambda_k}\ln\frac{\Delta_{\text{sat}}}{\Delta_k(T_{k+1})} = \frac{1}{\lambda_k}\ln\frac{(\alpha - 1)\lambda_k}{\epsilon},$$
$$\alpha = 2^{2/3}. \tag{22}$$

Figure 2 shows the result obtained averaging over 1000 initial perturbations. Scattered markers represent the values of $\Delta_1(T_k)$ at the different saturation times, obtained according to the quasilinear analysis. The agreement with the direct simulation of (14) is quite good. The global behavior can be fitted by a power law, whose slope can be roughly estimated by the following argument. From (22), one has that the periods M_k scale, apart from logarithmic corrections, as $M_k \sim \lambda_k^{-1} \sim \alpha^{-k}$. From (21) the growth of Δ_1 during period M_k is estimated to be $\sim \epsilon^k$. Then, we expect $\Delta_1(t) \sim t^\gamma$ with $\gamma = -\ln\epsilon/\ln\alpha$.
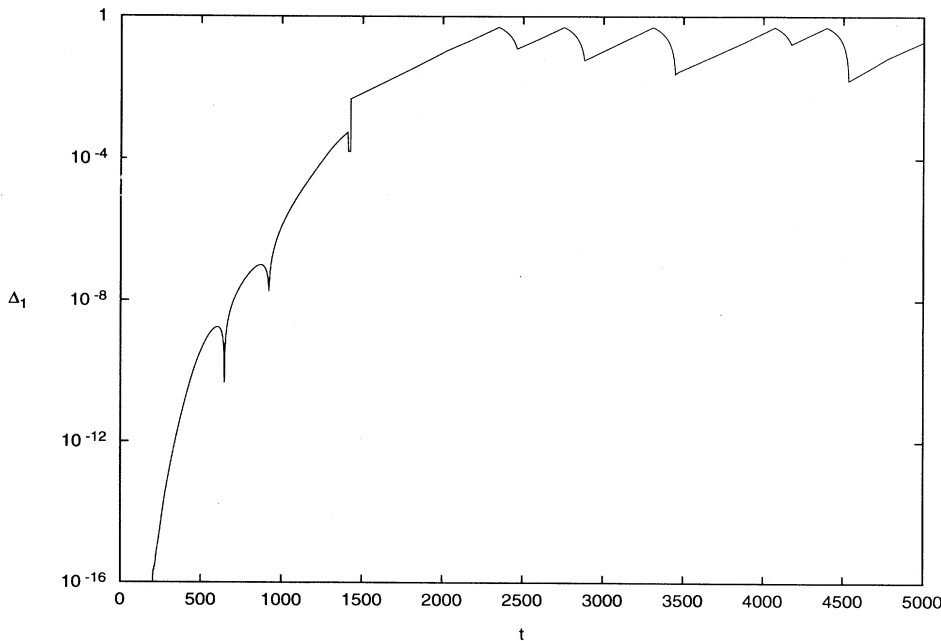

FIG. 1. Error growth Δ_1 as a function of t for $\epsilon = 10^{-4}$. The straight segments correspond to exponential growth driven by different dominant scales.
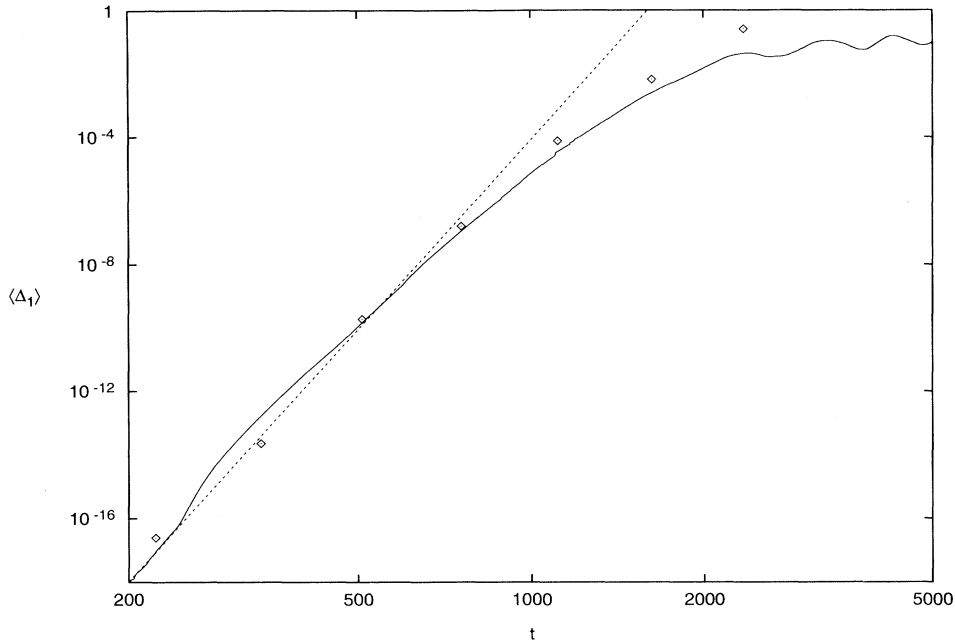
FIG. 2. Log-log plot of $\langle \Delta_1 \rangle$ as a function of t for $\epsilon = 10^{-4}$. The average is taken over 1000 initial configurations. The symbols (diamonds) are the estimated growth of the largest scale Δ_1 during different periods M_k according to the quasi-linear approximation. Dashed line: power law expected by the simple argument described in the text.

We have also performed a second numerical experiment with a stronger coupling $\epsilon = 10^{-2}$ and quadratic coupling function $f(x) = x^2$. The initial error is $\delta_0 = 10^{-3}$, while all the other parameters in the model are unchanged. We take an average of 1000 runs of 2000 steps in order to get a good statistics. The results are reported in Fig. 3, where one sees that the error on large scale $\Delta_1(t)$ has a complex behavior resulting from the combinations of several time scales, which are now not well separated.

However, even in this case, it is possible to determine an apparent power-law regime for intermediate times.

We stress that the above behaviors do not depend on the particular form of g_k, f, and λ_k. The system of coupled maps with different chaotic characteristic time teaches us that it is possible to have nontrivial time evolutions of *noninfinitesimal* perturbations at slowest scale, and that these can be fitted by power laws, although they are actually generated by saturation processes. In this
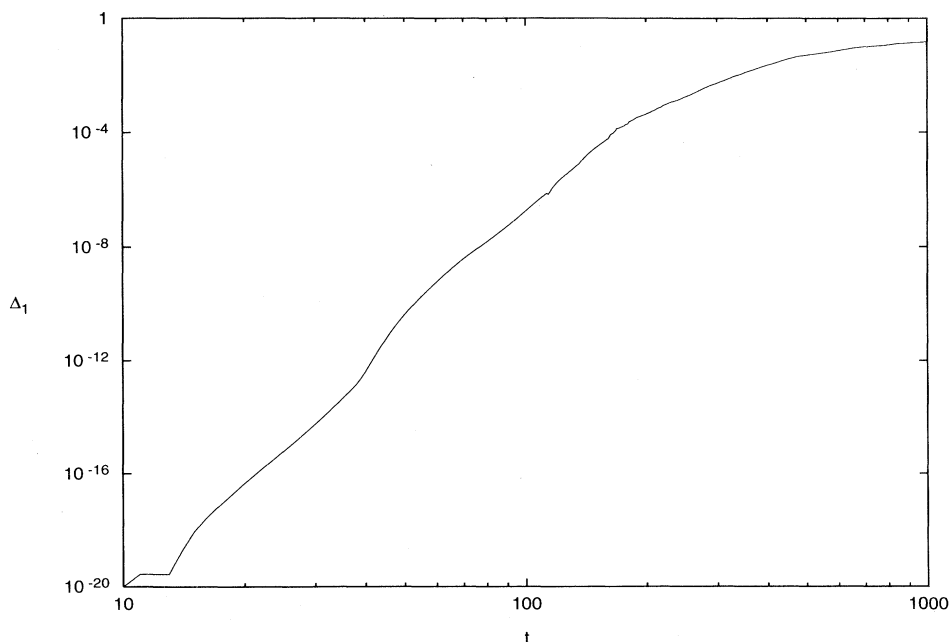

FIG. 3. Error growth Δ_1 for a nonlinearly coupled system with $\epsilon = 10^{-2}$.

kind of system, if we are interested in long-time predictions, the maximum Lyapunov exponent is of little or no importance and one should consider all the time scales present in the system.

IV. PREDICTABILITY IN A SHELL MODEL OF TURBULENCE

In this section we discuss the problem of predictability in a model for the energy cascade in three-dimensional fully developed turbulence [15–18]. The model, which is intended to mimic the Navier-Stokes equations, is defined in the Fourier space as follows. The Fourier space is divided into N shells labeled by the wave-vector modulus $k_n = k_0 2^n$, where k_0 is an arbitrary constant, each one containing all the wave vector $\mathbf{k}$ with modulus $k_0 2^n < |\mathbf{k}| \le k_0 2^{n+1}$. The velocity difference over the length scale $\sim k_n^{-1}$ is given by a complex variable u_n representing the Fourier components of the velocity field. The evolution is given by the set of N ordinary differential equations

$$\frac{d}{dt} u_n = -\nu k_n^2 u_n + i g_n + f_n, \qquad (23)$$

$$g_n = k_n u_{n+1}^* u_{n+2}^* - \frac{1}{2} k_{n-1} u_{n-1}^* u_{n+1}^*$$
$$- \frac{1}{2} k_{n-2} u_{n-2}^* u_{n-1}^*, \qquad (24)$$

where f_n is an external forcing, acting on large scale, necessary to have a stationary state, and ν is the viscosity. The main differences with the Navier-Stokes equations are (i) the wave vectors and the velocity fields u_n are scalars; (ii) there are only nearest- and next-nearest neighbor interactions among shells. The first point implies that it is not possible to have geometrical structures, all information on phases being lost. The second point does not represent a strong limitation as long as the energy cascade in Fourier space is local, with exponentially decreasing interactions among shells. This is rather sensible for three-dimensional turbulence, but not for the two-dimensional case [17].

Despite the fact that the time evolution governed by (23) and (24) spends long times around an unstable fixed point given by the Kolmogorov law $|u_n| \propto k_n^{-1/3}$ [18], it exhibits chaotic behavior on a strange attractor in the $2N$-dimensional phase space, with maximum Lyapunov exponent roughly proportional to $\nu^{-1/2}$. The velocity structure functions $\langle |u_n|^p \rangle \sim k_n^{-\zeta_p}$ have nonlinear exponents ζ_p very similar to those of real turbulence [16].

Our study of predictability is based on the comparison of the temporal evolution of pairs of different realizations of the velocity field, say u_n and v_n. Both fields evolve according to (23) and (24) form initial conditions such that (i) the energy spectra of u_n and v_n at the initial time are equal; (ii) u_n and v_n at initial time differ only on small scales, corresponding to wave number $k_n \ge k_{n_E}$:

$$v_n = \begin{cases} u_n & \text{for } n < n_E, \\ e^{i w_n} u_n & \text{for } n \ge n_E, \end{cases} \qquad (25)$$

where w_n is a random number uniformly distributed in the range $[0, \theta]$.

By changing the value of θ we can modify the correlation between the two fields. The extreme case $\theta = 2\pi$, i.e., completely uncorrelated variables for $n \ge n_E$, corresponding to the Lorenz choice discussed in Sec. II.

Previous works [6] investigated the growth of different small perturbations in shell models. Here we want to study this issue for a finite perturbation at initial time.

In the numerical simulation we have taken as the reference field u_n in (25) a solution of (23) and (24) obtained from a long simulation starting from a random initial condition. The forcing f_n was taken constant and equal to

$$f_n = (1 + i) \gamma \delta_{n,4} \qquad (26)$$

with $\gamma = 0.005$. The simulations were done mainly for two different systems: (A) $N = 19$ and $\nu = 10^{-6}$; (B) $N = 27$ and $\nu = 10^{-9}$. We used the leap-frog method of integration with time step 10^{-3} in the case (A) and 2×10^{-5} in the case (B). The average is over 10^3 different realizations of the field v_n. All the figures will be for the case (A), the case (B) being similar.

In order to understand whether intermittency has any effect on the qualitative features, we also performed a detailed study in terms of closure approximation, where, by construction, one considers averaged quantities neglecting intermittency. We thus developed the standard eddy damped quasinormal Markovian (EDQNM) approximation [14] for the shell model (see Appendixes A and B).

Among the various quantities that can be computed, we focused on the error spectrum at wave vector k_n,

$$\Delta_n = \tfrac{1}{2} \langle (u_n - v_n)(u_n^* - v_n^*) \rangle = (E_n - \operatorname{Re} W_n), \qquad (27)$$

where $E_n = \langle u_n u_n^* \rangle = \langle v_n v_n^* \rangle$ is the energy of the two fields and $W_n = \langle u_n v_n^* \rangle$ is the overlap energy at scale n.

In Figs. 4 and 5 the error energy spectrum Δ_n is showed at different times for $\theta = 2\pi$ and 10^{-4}, respectively.

In Fig. 4 we see that at the beginning we have a very fast growth until Δ_n reaches the saturation (i.e., $\Delta_n = E_n$) at large n. Then one has a sort of inverse cascade on the error. This is also the main feature one observes in the case of strong initial perturbation (Fig. 5).

In order to compare the error growth in the shell model with the behavior observed in the toy model of Sec. III, we also compute the (global) growth of the large-scale error

$$\delta U_0 = \left[\frac{\Delta_6 + \Delta_7 + \Delta_8}{3} \right]^{1/2} \qquad (28)$$

and the moments of the difference field, defined as

$$\langle |\delta u|^q \rangle = \left\langle \left[\sum_n 2\Delta_n \right]^{q/2} \right\rangle. \qquad (29)$$

Figures 6 and 7 show the growth of the moments of $\langle |\delta u|^q \rangle^{1/q}$, respectively, for $\theta = 2\pi$ and $\theta = 10^{-4}$. For the first case we observe at intermediate times a
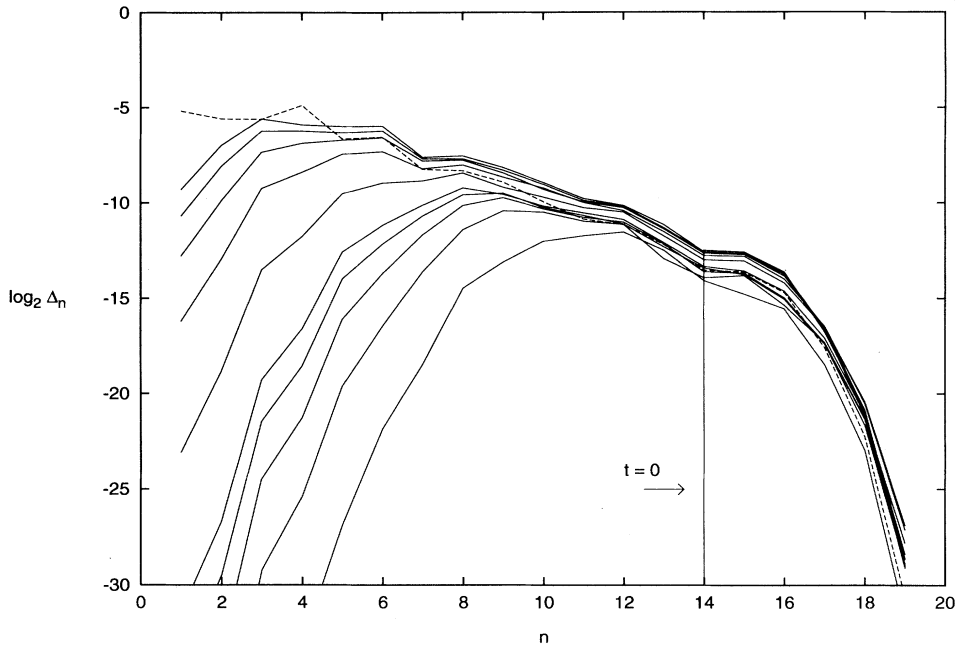
FIG. 4. Error spectrum Δ_n as a function of n at different time for case (A) and $\theta = 2\pi$. The lines are taken at times 0, 1, 2, 3, 4, 5, 10, 15, 20, 25, and 30 sec after the perturbation has been done. The dashed line is the spectrum E_n.

power-law behavior in agreement with the Lorenz prediction. The intermittency produces anomalous scaling, i.e., $\langle |\delta u|^q \rangle \sim t^{q\alpha(q)}$ where $\alpha(q)$ is a nonincreasing function of q. From Fig. 6 we have a rather fair evidence of anomalous scaling. However, in our opinion, the precise values of the scaling exponents may be a problem interesting in itself but not too important, at least at a qualitative level, in the issue of the predictability. Here the relevant aspect is the fact that growth of physical perturbations evolves according to a nonexponential law, as

for infitesimal perturbations. Let us note that the value of $\alpha(2)$ seems to be close to $1/2$ as in the Lorenz prediction where no intermittent effects are taken into account. In the case of small initial perturbation (Fig. 7) one can recognize an initial exponential growth until the error saturates at small scales. Then we find a kind of power-law behavior.

For a qualitative comparison with the results discussed for the coupled maps, we show in Fig. 8 the growth of δU_0. We can recognize an initial exponential growth
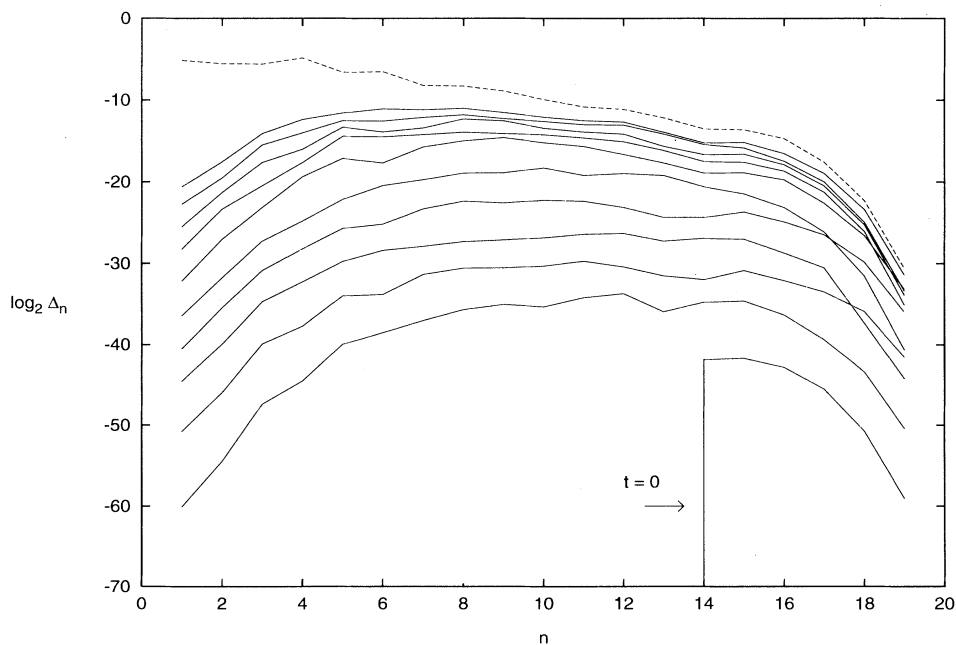

FIG. 5. Error spectrum Δ_n as a function of n at different time for case (A) and $\theta = 10^{-4}$. The lines are taken at times 0, 5, 10, 15, 20, 25, 30, 35, 40, 45, and 50 sec after the perturbation has been done. The dashed line is the spectrum E_n.
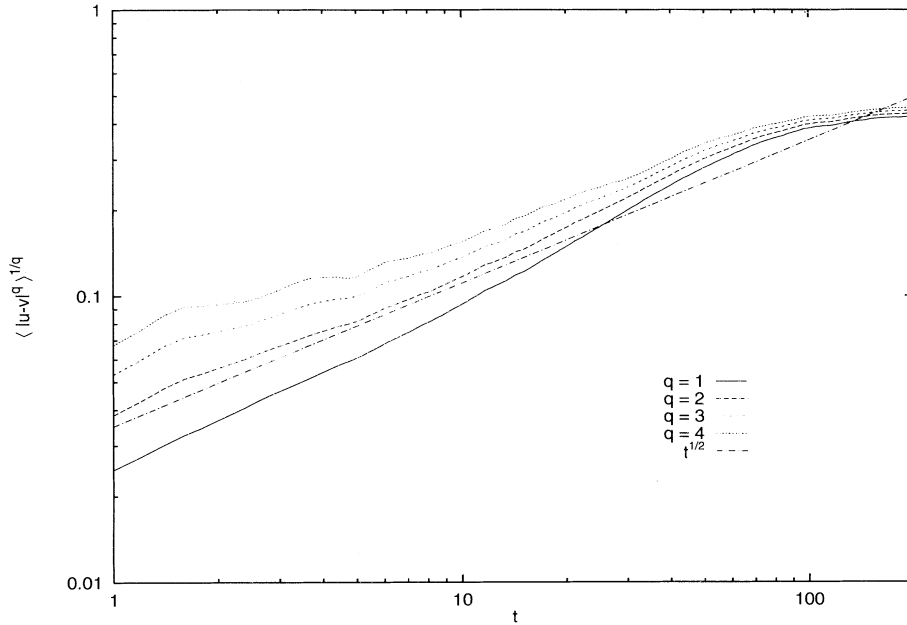
FIG. 6. Moments of the difference field $\langle|\delta u|^q\rangle^{1/q}$ $(q = 1, 2, 3, 4)$ as a function of t for case (A) and $\theta = 2\pi$.

driven by the smallest scale; in later times all the time scales interplay leading to a nonsimple function which can be misinterpreted as a power law.

The closure approximation for the shell model leads to a qualitative similar behavior. Of course, in this approach $\langle|\delta u|^q\rangle = C_q \langle|\delta u|\rangle^q$ by construction, so intermittency effects cannot be detected.

The basic idea of closure is quite straightforward: one writes a Reynolds hierarchy for the moments of the shell variables, and truncates the chain of equations at the lowest sensible order. The full derivation is given below in Appendixes A and B. The closure equation thus gives information on the behavior of E_n and W_n as functions of time. The results are similar to those obtained by
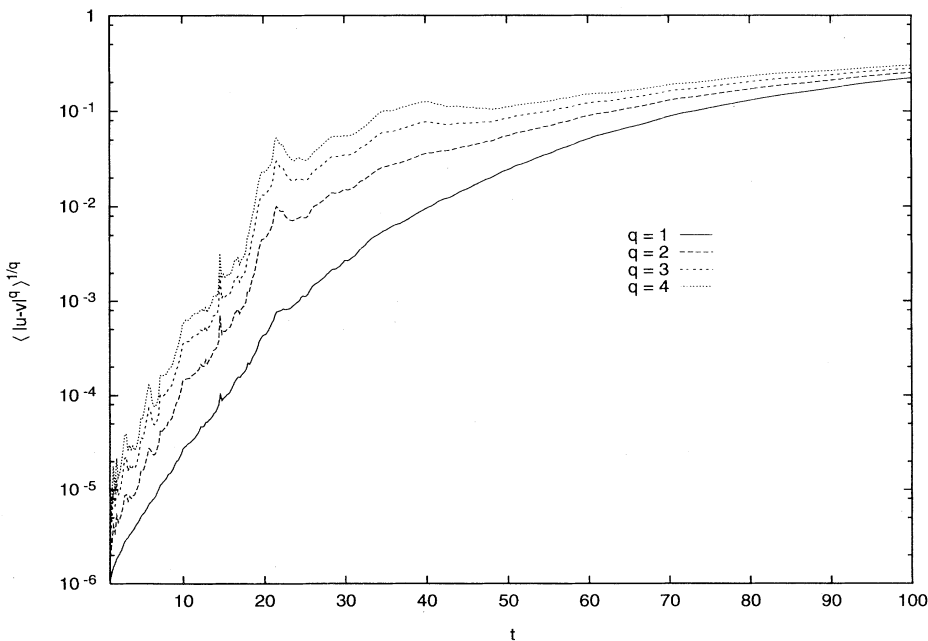

FIG. 7. Moments of the difference field $\langle|\delta u|^q\rangle^{1/q}$ $(q = 1, 2, 3, 4)$ as a function of t for case (A) and $\theta = 10^{-4}$.
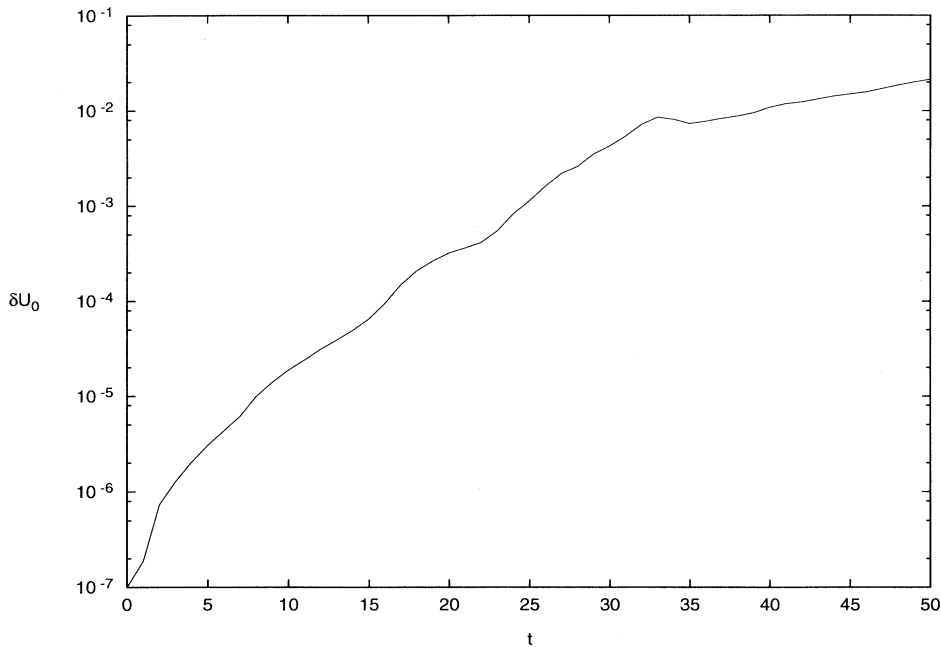
FIG. 8. δU_0 as a function of t for case (A).

the direct integration (and ensemble average) of the shell model, as is evident by the direct comparison of Fig. 9 with Fig. 4 and Fig. 10 with Fig. 5. This is clear evidence that the relevant mechanism, at least at a qualitative level, is due to the existence of many characteristic times and not to intermittency effects.

V. DISCUSSION

The predictability problem can be formulated in terms of the Lyapunov exponent, or the effective Lyapunov exponent, only for infinitesimal perturbations. On the
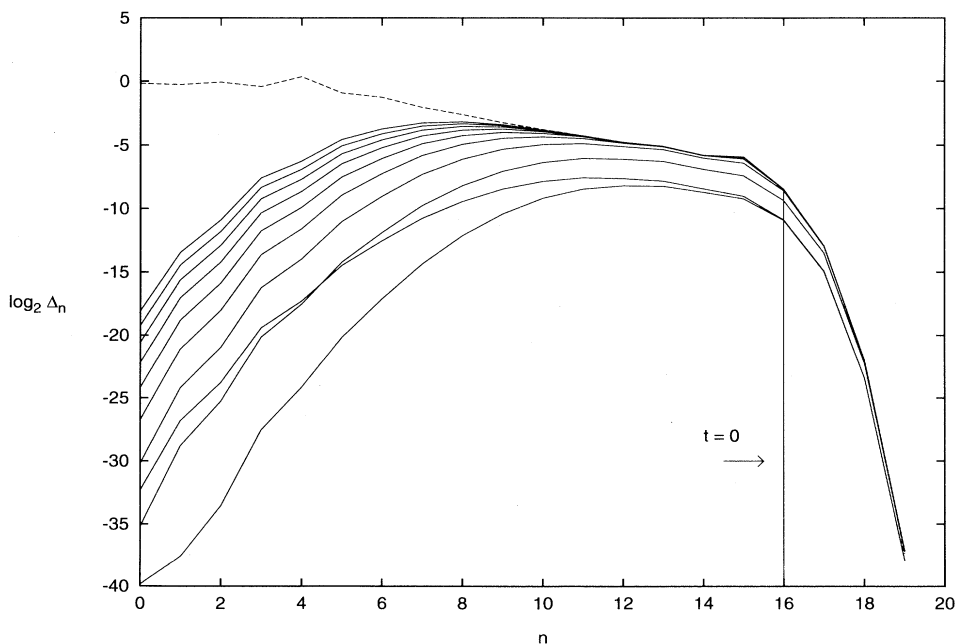

FIG. 9. Error spectrum Δ_n as a function of n at different time for the EDQNM approximation and $\theta = 10^{-4}$. The lines are taken at time interval 0.02 sec from the perturbation, first line. The dashed line is the spectrum E_n.
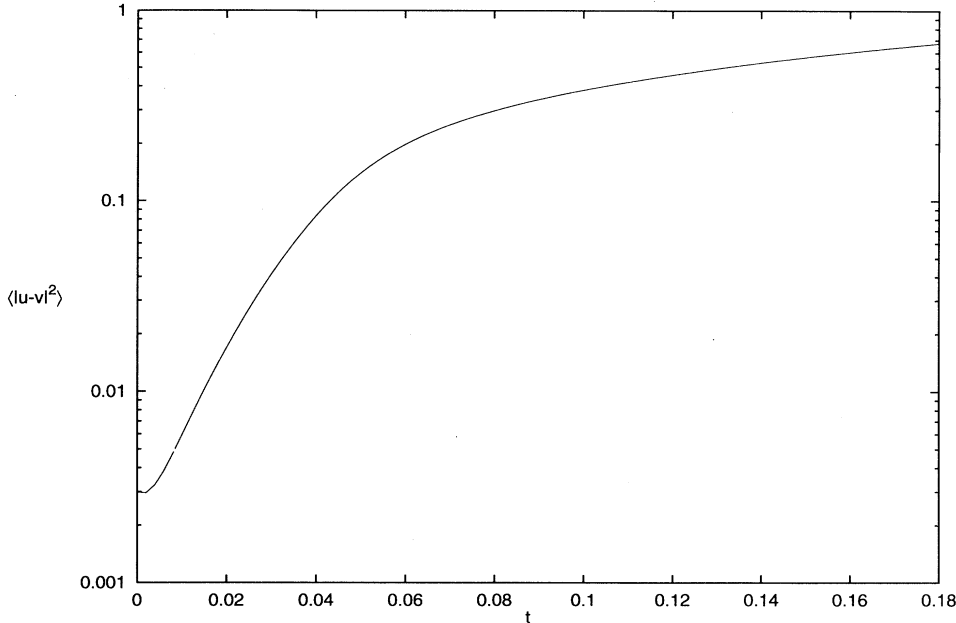
FIG. 10. $\langle |\delta u|^2 \rangle$ as a function of n at different time for the EDQNM approximation and $\theta = 10^{-4}$.

other hand, in systems with many different characteristic times and finite perturbations the nonlinear effects are very relevant. A direct consequence is that the growth of the perturbation is, apart at very short times, not exponential but rather similar to a power law. Actually it is a sequence of exponentials with varying rates. This mechanism has an important practical relevance: the predictability time for finite perturbations can be much larger than the inverse of the Lyapunov exponent (1).

For example, in three-dimensional turbulence for a "physical" perturbation localized at the initial time at the Kolmogorov length η, $\delta v = O(v(\eta))$, the predictability time is $T \sim L/V$, independent of the Reynolds number. On the contrary, the predictability time for an infinitesimal perturbation is proportional to the inverse of the maximum Lyapunov exponent λ, which grows as a power of the Reynolds number. Hence the predictability time decreases for increasing Re.

These results give a strong indication that despite the presence of strong chaos, realistic situations have relatively long predictability times.

In conclusion we have showed that the concepts of Lyapunov exponents, effective Lyapunov exponent, and Kolmogorov entropy give insufficient information on the chaotic behavior of extended systems.

ACKNOWLEDGMENTS

APPENDIX A

Here we derive the equations for the energy of the field in the eddy damped quasinormal Markovian approximation (EDQNM) for the shell model. For more details see, e.g., [14,19].

We are interested into the energy of the shell n given by $E_n = \langle u_n u_n^* \rangle$. Differentiation with respect to time of E_n, and use of (23) and (24), leads to the evolution equation for E_n for the shell model:

$$\frac{d}{dt}E_n = -2\nu k_n^2 E_n + i\langle g_n u_n^* \rangle - i\langle u_n g_n^* \rangle + 2\epsilon \delta_{n,4}.$$

$$(A1)$$

In order to have a constant energy input ϵ we assumed a forcing

$$f_n = \frac{u_n}{|u_n|^2} \epsilon \delta_{n,4} \qquad (A2)$$

in (23). Equation (A1) is not closed since the third and fourth terms on the rhs involve third-order correlation functions. For example

$$\langle g_n u_n^* \rangle = k_n \langle u_n^* u_{n+1}^* u_{n+2}^* \rangle - \tfrac{1}{2} k_{n-1} \langle u_{n-1}^* u_n^* u_{n+1}^* \rangle$$
$$- \tfrac{1}{2} k_{n-2} \langle u_{n-2}^* u_{n-1}^* u_n^* \rangle \qquad (A3)$$

and similarly the other. The third-order cumulants obey a differential equation involving fourth-order correlation functions, e.g.,

$$\frac{d}{dt}\langle u_n \, u_{n+1} \, u_{n+2}\rangle$$

$$= -\nu\,(k_n^2 + k_{n+1}^2 + k_{n+2}^2)\langle u_n \, u_{n+1} \, u_{n+2}\rangle$$

$$+i\langle g_n \, u_{n+1} \, u_{n+2}\rangle$$

$$+i\langle u_n \, g_{n+1} \, u_{n+2}\rangle + i\langle u_n \, u_{n+1} \, g_{n+2}\rangle, \qquad \text{(A4)}$$

and so on. Thus in order to have a closed problem we have to truncate the hierarchy. This is done assuming a quasinormal probability distribution for the field, and factorizing the fourth-order correlation functions as

$$\langle x_1 \, x_2 \, x_3 \, x_4\rangle = \langle x_1 \, x_2\rangle \, \langle x_3 \, x_4\rangle + \langle x_1 \, x_3\rangle \, \langle x_2 \, x_4\rangle$$

$$+ \langle x_1 \, x_4\rangle \, \langle x_3 \, x_2\rangle. \qquad \text{(A5)}$$

By means of (A5), and the assumption of isotropic turbulence

$$\langle u_n \, u_m^*\rangle = \delta_{nm} \, E_n, \quad \langle u_n \, u_m\rangle = 0, \qquad \text{(A6)}$$

it is easy to evaluate the terms involving the fourth-order correlation functions in the equations for the third-order ones, and close the hierarchy. For example, for Eq. (A4) we have

$$\begin{aligned} \langle g_n \, u_{n+1} \, u_{n+2}\rangle &= k_n \, E_{n+1} \, E_{n+2}, \\ \langle u_n \, g_{n+1} \, u_{n+2}\rangle &= -\tfrac{1}{2} \, k_n \, E_n \, E_{n+2}, \\ \langle u_n \, u_{n+1} \, g_{n+2}\rangle &= -\tfrac{1}{2} \, k_n \, E_n \, E_{n+1}. \end{aligned} \qquad \text{(A7)}$$

Inserting (A7) into (A4) we obtain

$$\left[\frac{d}{dt} + \nu(k_n^2 + k_{n+1}^2 + k_{n+2}^2)\right] \langle u_n \, u_{n+1} \, u_{n+2}\rangle = iS(n,t) \qquad \text{(A8)}$$

with

$$S(n,t) = k_n \, E_{n+1} \, E_{n+2} - \tfrac{1}{2} \, k_n \, E_n \, E_{n+2} - \tfrac{1}{2} \, k_n \, E_n \, E_{n+1}. \qquad \text{(A9)}$$

Similar equations hold for the third-order cumulants entering into Eq. (A3).

The quasinormal approximation (A8) is known to give unphysical results [19]. In particular it does not produce positive definite energy spectra. The problem has been cured by introducing the so-called "eddy damped" approximation. One replaces (A8) with

$$\left[\frac{d}{dt} + \nu(k_n^2 + k_{n+1}^2 + k_{n+2}^2) \right.$$

$$\left. + \mu_n + \mu_{n+1} + \mu_{n+2}\right] \langle u_n \, u_{n+1} \, u_{n+2}\rangle = iS(n,t), \qquad \text{(A10)}$$

where

$$\mu_n \equiv \mu(k_n, E_n) = \alpha \, k_n \, E_n^{1/2}. \qquad \text{(A11)}$$

Dimensionally $k_n E_n^{1/2}$ is an inverse time, the turnover time at shell n. We have one free parameter, the dimensionless constant α. It should be adjusted such that the spectrum is as similar as possible to the spectrum obtained in simulations of the full equation. We will return to this point later.

Equation (A10) can be easily integrate, and the solution reads

$$\langle u_n \, u_{n+1} \, u_{n+2}\rangle = i \int_0^t dt' \, e^{-[\nu(k_n^2 + k_{n+1}^2 + k_{n+2}^2) + \mu_n + \mu_{n+1} + \mu_{n+2}]\,(t-t')} \, S(n,t'). \qquad \text{(A12)}$$

It has been proved that if we assume that $S(n,t)$ does not vary significantly in the range where the exponential in (A12) is substantially different from zero, then this is a sufficient condition for the positiveness of the energy spectra [19]. This assumption is called Markovianization. Therefore the third-order correlation function at time t in the EDQNM approximation reads

$$\langle u_n \, u_{n+1} \, u_{n+2}\rangle = i\theta(n,t) \, S(n,t), \qquad \text{(A13)}$$

where

$$\theta(n,t) = \int_0^t dt' \, e^{-[\nu(k_n^2 + k_{n+1}^2 + k_{n+2}^2) + \mu_n + \mu_{n+1} + \mu_{n+2}]\,(t-t')}$$

$$= \frac{1 - e^{-[\nu(k_n^2 + k_{n+1}^2 + k_{n+2}^2) + \mu_n + \mu_{n+1} + \mu_{n+2}]\,t}}{\nu(k_n^2 + k_{n+1}^2 + k_{n+2}^2) + \mu_n + \mu_{n+1} + \mu_{n+2}}. \qquad \text{(A14)}$$

Similar equations hold for the other third-order correlation functions.

We can now go back to (A1) and write down the equation for the energy E_n in the EDQNM approximation,

$$\left(\frac{d}{dt} + 2\nu k_n^2\right) E_n = 2\Big[k_n \, \theta(n,t) \, S(n,t)$$

$$-\tfrac{1}{2} \, k_{n-1} \, \theta(n-1,t) \, S(n-1,t)$$

$$-\tfrac{1}{2} \, k_{n-2} \, \theta(n-2,t) \, S(n-2,t)\Big]$$

$$+2\,\epsilon\,\delta_{n,4}. \qquad \text{(A15)}$$

The quasinormal ansatz implies the absence of intermittency corrections. This is an essential limitation of all closure theories. The energy spectrum of the shell model in the EDQNM approximation must therefore obey $E_n \simeq C(\alpha)\epsilon^{2/3} k_n^{-2/3}$ in the inertial range. The un-

determined function $C(\alpha)$ is the Kolmogorov constant.

On the other hand, it has become clear in several independent investigations that intermittency corrections exist in shell models. The energy spectrum is therefore in reality more closely described by $E_n \sim F(\epsilon) k_n^{-\zeta_2}$, where the exponent ζ_2 has been estimated to be 0.70 [16]. The function F that gives the prefactor to the power law in the inertial range should not depend on viscosity, but depends on the forcing through ϵ, the mean dissipation of energy per unit time, or, equivalently, the mean energy input into the system from the force. In a really large inertial range the two power laws are not good approximations to the one other. The best that can be done is to demand that the spectra agree as closely as possible at the upper end of the inertial range. The disagreement at the lower end will then be approximately $(k_L/k_0)^{\zeta_2-2/3}$. This is not a very large discrepancy. Assuming an inertial range of 20 shells, that is, a scale separation of 10^6, and $\zeta_2 = 0.70$, the mismatch is only a factor 1.5. In practice a number of α's have been tried and the two spectra compared until a reasonable agreement is achieved. For $\alpha = 0.06$ we obtain $C(\alpha) = 1.5$, which is the value observed both in simulations of the shell model and in experiments [19].

APPENDIX B

Here we derive the equations for the energy of the field difference in the eddy damped quasinormal Markovian approximation (EDQNM) for the shell model. The procedure is similar to that described in Appendix A for the energy, so we only report the main equations.

We consider two independent realizations of the field, u_n and v_n, with the same energy spectrum E_n, both evolving according to (23) and (24). For simplicity of notation, the equation of motion of the field v_n is rewritten as

$$
\begin{aligned}
\frac{d}{dt} v_n &= -\nu k_n^2 + i h_n + \tilde{f}_n, \\
h_n &= k_n v_{n+1}^* v_{n+2}^* - \tfrac{1}{2} k_{n-1} v_{n-1}^* v_{n+1}^* \\
&\quad - \tfrac{1}{2} k_{n-2} v_{n-2}^* v_{n-1}^*, \\
\tilde{f}_n &= \frac{v_n}{|v_n|^2} \epsilon \delta_{n,4}.
\end{aligned}
\tag{B1}
$$

We are interested into the energy of the field difference at the shell n,

$$
\Delta_n = \tfrac{1}{2} \langle (u_n - v_n)(u_n^* - v_n^*) \rangle = (E_n - \mathrm{Re}\, W_n), \quad \text{(B2)}
$$

where $W_n = \langle u_n v_n^* \rangle$. The evolution equation of W_n is easily derived by differentiation with respect to time and reads

$$
\frac{d}{dt} W_n = -2\nu k_n^2 W_n + i\langle g_n v_n^* \rangle - i\langle u_n h_n^* \rangle + 2\epsilon \delta_{n,4}.
\tag{B3}
$$

As in the case of E_n, this equation is not closed since it involves third-order cumulants of u_n and v_n. For example,

$$
\begin{aligned}
\langle g_n v_n^* \rangle &= k_n \langle v_n^* u_{n+1}^* u_{n+2}^* \rangle - \tfrac{1}{2} k_{n-1} \langle u_{n-1}^* v_n^* u_{n+1}^* \rangle \\
&\quad - \tfrac{1}{2} k_{n-2} \langle u_{n-2}^* u_{n-1}^* v_n^* \rangle
\end{aligned}
\tag{B4}
$$

and similarly the other. As done for the energy E_n, the hierarchy is closed for the fourth-order correlation functions. With a calculation similar to that of Appendix A, one obtains

$$
\left[\frac{d}{dt} + \nu(k_n^2 + k_{n+1}^2 + k_{n+2}^2) \right] \langle v_n^* u_{n+1}^* u_{n+2}^* \rangle
$$

$$
\begin{aligned}
&= -i k_n W_{n+1}^* W_{n+2}^* + i\tfrac{1}{2} k_n W_n E_{n+2} \\
&\quad + i\tfrac{1}{2} k_n W_n E_{n+1}
\end{aligned}
\tag{B5}
$$

and similar equations for the others.

We then perform the eddy damped and Markovian approximation, i.e., add a damping term $(\mu_n + \mu_{n+1} + \mu_{n+2})W_n$ to the lhs, where μ_n is given by (A11), and we integrate the resulting equation in the Markovian approximation—see Appendix A for more details. From (B5), it follows

$$
\begin{aligned}
\langle v_n^* u_{n+1}^* u_{n+2}^* \rangle &= -i\theta(n,t) k_n \big[k_n W_{n+1}^* W_{n+2}^* \\
&\quad - \tfrac{1}{2} k_n W_n E_{n+2} - \tfrac{1}{2} k_n W_n E_{n+1} \big]
\end{aligned}
\tag{B6}
$$

with $\theta(n,t)$ given by (A14). The other cumulants lead to similar equations. Collecting all the terms one finally obtains the equation for W_n in the EDQNM approximation,

$$
\begin{aligned}
\left(\frac{d}{dt} + 2\nu k_n^2 \right) W_n &= 2\Big[k_n^2 \theta(n,t) \left(W_{n+1}^* W_{n+2}^* - \tfrac{1}{2} W_n E_{n+2} - \tfrac{1}{2} W_n E_{n+1} \right) \\
&\quad - \tfrac{1}{2} k_{n-1}^2 \theta(n-1,t) \left(W_n E_{n+1} - \tfrac{1}{2} W_{n-1}^* W_{n+1}^* - \tfrac{1}{2} E_{n-1} W_n \right) \\
&\quad - \tfrac{1}{2} k_{n-2}^2 \theta(n-2,t) \left(E_{n-1} W_n - \tfrac{1}{2} E_{n-2} W_n - \tfrac{1}{2} W_{n-2}^* W_{n-1}^* \right) \Big] \\
&\quad + 2\epsilon \delta_{n,4}.
\end{aligned}
\tag{B7}
$$

[1] E. N. Lorenz, J. Atmos. Sci. **20**, 130 (1963).

[2] G. Benettin, L. Galgani, A. Giorgilli, and J. M. Strelcyn, Meccanica **15**, 9 (1980); **15**, 20 (1980).

[3] G. Paladin and A. Vulpiani, Phys. Rep. **156**, 147 (1987).

[4] A. Pikovsky, Chaos **3**, 225 (1993).

[5] G. Paladin and A. Vulpiani, J. Phys. A **27**, 4911 (1994).

[6] A. Crisanti, M. H. Jensen, G. Paladin, and A. Vulpiani, J. Phys. A **26**, 6943 (1993).

[7] A. Crisanti, M. H. Jensen, G. Paladin, and A. Vulpiani, Phys. Rev. Lett. **70**, 166 (1993)

[8] D. Ruelle, Phys. Lett. **72A**, 81 (1979).

[9] G. Parisi and U. Frisch, in *Turbulence and Predictability in Geophysical Flows and Climatic Dynamics*, edited by N. Ghil, R. Benzi, and G. Parisi (North-Holland, Amsterdam, 1985).

[10] R. Benzi, G. Paladin, G. Parisi, and A. Vulpiani, J. Phys. A **17**, 3521 (1984).

[11] E. N. Lorenz, Tellus **21**, 3 (1969).

[12] D. K. Lilly, *Dynamic Meteorology*, edited by P. Morel (Riedel, Boston, 1973).

[13] C. E. Leith and R. H. Kraichnan, J. Atmos. Sci. **29**, 1041 (1972).

[14] M. Lesieur, *Turbulence in Fluids* (Kluwer, Dordrecht, 1993).

[15] M. Yamada and K. Ohkitani, J. Phys. Soc. Jpn. **56**, 4210 (1987).

[16] M. H. Jensen, G. Paladin, and A. Vulpiani, Phys. Rev. A **43**, 798 (1991).

[17] E. Aurell, G. Boffetta, A. Crisanti, P. Frick, G. Paladin, and A. Vulpiani, Phys. Rev. E **50**, 4705 (1994).

[18] L. Biferale, A. Lambert, R. Lima, and G. Paladin, Physica D **80**, 105 (1995).

[19] S. A. Orszag, in *Fluid Dynamics*, edited by R. Balian and J. L. Peuble (Gordon and Breach, London, 1977).